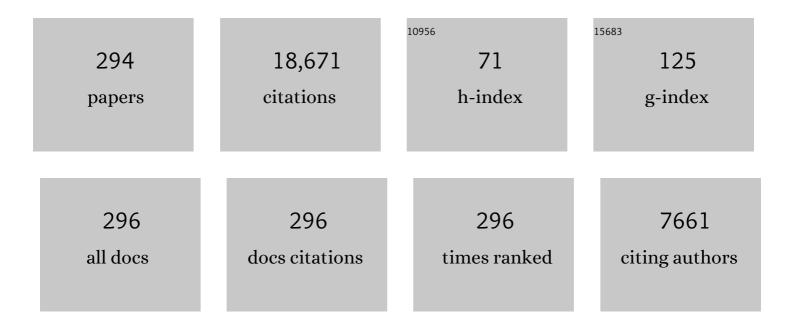
## Mikhail L Zheludkevich

List of Publications by Year in descending order

Source: https://exaly.com/author-pdf/7017344/publications.pdf Version: 2024-02-01



#	Article	IF	CITATIONS
1	Layer-by-Layer Assembled Nanocontainers for Self-Healing Corrosion Protection. Advanced Materials, 2006, 18, 1672-1678.	11.1	653
2	Anticorrosion Coatings with Self-Healing Effect Based on Nanocontainers Impregnated with Corrosion Inhibitor. Chemistry of Materials, 2007, 19, 402-411.	3.2	556
3	Nanostructured sol–gel coatings doped with cerium nitrate as pre-treatments for AA2024-T3. Electrochimica Acta, 2005, 51, 208-217.	2.6	498
4	Active protection coatings with layered double hydroxide nanocontainers of corrosion inhibitor. Corrosion Science, 2010, 52, 602-611.	3.0	456
5	Sol–gel coatings for corrosion protection of metals. Journal of Materials Chemistry, 2005, 15, 5099.	6.7	454
6	Plasma electrolytic oxidation coatings with particle additions – A review. Surface and Coatings Technology, 2016, 307, 1165-1182.	2.2	408
7	Active Anticorrosion Coatings with Halloysite Nanocontainers. Journal of Physical Chemistry C, 2008, 112, 958-964.	1.5	340
8	"Smart―coatings for active corrosion protection based on multi-functional micro and nanocontainers. Electrochimica Acta, 2012, 82, 314-323.	2.6	340
9	Triazole and thiazole derivatives as corrosion inhibitors for AA2024 aluminium alloy. Corrosion Science, 2005, 47, 3368-3383.	3.0	324
10	Mechanism of Corrosion Inhibition of AA2024 by Rare-Earth Compounds. Journal of Physical Chemistry B, 2006, 110, 5515-5528.	1.2	315
11	Enhancement of Active Corrosion Protection via Combination of Inhibitor-Loaded Nanocontainers. ACS Applied Materials & Interfaces, 2010, 2, 1528-1535.	4.0	302
12	High effective organic corrosion inhibitors for 2024 aluminium alloy. Electrochimica Acta, 2007, 52, 7231-7247.	2.6	287
13	Nanoporous titania interlayer as reservoir of corrosion inhibitors for coatings with self-healing ability. Progress in Organic Coatings, 2007, 58, 127-135.	1.9	280
14	Novel Inorganic Host Layered Double Hydroxides Intercalated with Guest Organic Inhibitors for Anticorrosion Applications. ACS Applied Materials & 2009; Interfaces, 2009, 1, 2353-2362.	4.0	277
15	Role of intermetallic phases in localized corrosion of AA5083. Electrochimica Acta, 2007, 52, 7651-7659.	2.6	267
16	Evaluation of self-healing ability in protective coatings modified with combinations of layered double hydroxides and cerium molibdate nanocontainers filled with corrosion inhibitors. Electrochimica Acta, 2012, 60, 31-40.	2.6	263
17	Corrosion protective properties of nanostructured sol–gel hybrid coatings to AA2024-T3. Surface and Coatings Technology, 2006, 200, 3084-3094.	2.2	253
18	Novel hybrid sol–gel coatings for corrosion protection of AZ31B magnesium alloy. Electrochimica Acta, 2008, 53, 4773-4783.	2.6	253

#	Article	IF	CITATIONS
19	Zn–Al layered double hydroxides as chloride nanotraps in active protective coatings. Corrosion Science, 2012, 55, 1-4.	3.0	242
20	Plasma electrolytic oxidation coatings on Mg alloy with addition of SiO2 particles. Electrochimica Acta, 2016, 187, 20-33.	2.6	219
21	CeO2-filled sol–gel coatings for corrosion protection of AA2024-T3 aluminium alloy. Corrosion Science, 2009, 51, 2304-2315.	3.0	217
22	Comprehensive screening of Mg corrosion inhibitors. Corrosion Science, 2017, 128, 224-240.	3.0	206
23	Silica nanocontainers for active corrosion protection. Nanoscale, 2012, 4, 1287.	2.8	205
24	Mg-Ca binary alloys as anodes for primary Mg-air batteries. Journal of Power Sources, 2018, 396, 109-118.	4.0	193
25	Hydroxyapatite Microparticles as Feedback-Active Reservoirs of Corrosion Inhibitors. ACS Applied Materials & Interfaces, 2010, 2, 3011-3022.	4.0	187
26	Electrochemical study of inhibitor-containing organic–inorganic hybrid coatings on AA2024. Corrosion Science, 2009, 51, 1012-1021.	3.0	186
27	Influence of inhibitor addition on the corrosion protection performance of sol–gel coatings on AA2024. Progress in Organic Coatings, 2008, 63, 352-361.	1.9	181
28	Oxide nanoparticle reservoirs for storage and prolonged release of the corrosion inhibitors. Electrochemistry Communications, 2005, 7, 836-840.	2.3	177
29	Nanostructured LDH-container layer with active protection functionality. Journal of Materials Chemistry, 2011, 21, 15464.	6.7	174
30	The use of pre-treatments based on doped silane solutions for improved corrosion resistance of galvanised steel substrates. Surface and Coatings Technology, 2006, 200, 4240-4250.	2.2	167
31	The corrosion resistance of hot dip galvanised steel and AA2024-T3 pre-treated with bis-[triethoxysilylpropyl] tetrasulfide solutions doped with Ce(NO3)3. Corrosion Science, 2006, 48, 3740-3758.	3.0	155
32	Inhibitor-doped sol–gel coatings for corrosion protection of magnesium alloy AZ31. Surface and Coatings Technology, 2010, 204, 1479-1486.	2.2	155
33	Selecting medium for corrosion testing of bioabsorbable magnesium and other metals – A critical review. Corrosion Science, 2020, 171, 108722.	3.0	152
34	Complex anticorrosion coating for ZK30 magnesium alloy. Electrochimica Acta, 2009, 55, 131-141.	2.6	145
35	The effect of iron re-deposition on the corrosion of impurity-containing magnesium. Physical Chemistry Chemical Physics, 2016, 18, 1279-1291.	1.3	140
36	Self-healing protective coatings with "green―chitosan based pre-layer reservoir of corrosion inhibitor. Journal of Materials Chemistry, 2011, 21, 4805.	6.7	134

#	Article	IF	CITATIONS
37	Influence of preparation conditions of Layered Double Hydroxide conversion films on corrosion protection. Electrochimica Acta, 2014, 117, 164-171.	2.6	134
38	On the application of electrochemical impedance spectroscopy to study the self-healing properties of protective coatings. Electrochemistry Communications, 2007, 9, 2622-2628.	2.3	123
39	The synergistic combination of bis-silane and CeO2·ZrO2 nanoparticles on the electrochemical behaviour of galvanised steel in NaCl solutions. Electrochimica Acta, 2008, 53, 5913-5922.	2.6	120
40	Monitoring local spatial distribution of Mg2+, pH and ionic currents. Electrochemistry Communications, 2008, 10, 259-262.	2.3	118
41	Localized electrochemical study of corrosion inhibition in microdefects on coated AZ31 magnesium alloy. Electrochimica Acta, 2010, 55, 5401-5406.	2.6	117
42	TiOx self-assembled networks prepared by templating approach as nanostructured reservoirs for self-healing anticorrosion pre-treatments. Electrochemistry Communications, 2006, 8, 421-428.	2.3	116
43	Chitosan-based self-healing protective coatings doped with cerium nitrate for corrosion protection of aluminum alloy 2024. Progress in Organic Coatings, 2012, 75, 8-13.	1.9	116
44	Solâ€Gel/Polyelectrolyte Active Corrosion Protection System. Advanced Functional Materials, 2008, 18, 3137-3147.	7.8	115
45	Modification of bis-silane solutions with rare-earth cations for improved corrosion protection of galvanized steel substrates. Progress in Organic Coatings, 2006, 57, 67-77.	1.9	109
46	Insights into plasma electrolytic oxidation treatment with particle addition. Corrosion Science, 2015, 101, 201-207.	3.0	107
47	The corrosion resistance of hot dip galvanized steel pretreated with Bis-functional silanes modified with microsilica. Surface and Coatings Technology, 2006, 200, 2875-2885.	2.2	103
48	Corrosion protection properties of inhibitor containing hybrid PEO-epoxy coating on magnesium. Corrosion Science, 2018, 140, 99-110.	3.0	103
49	A new concept for corrosion inhibition of magnesium: Suppression of iron re-deposition. Electrochemistry Communications, 2016, 62, 5-8.	2.3	100
50	The role of individual components of simulated body fluid on the corrosion behavior of commercially pure Mg. Corrosion Science, 2019, 147, 81-93.	3.0	97
51	Corrosion protection of AA2024-T3 by LDH conversion films. Analysis of SVET results. Electrochimica Acta, 2016, 210, 215-224.	2.6	96
52	Mutual interplay of ZnO micro- and nanowires and methylene blue during cyclic photocatalysis process. Journal of Environmental Chemical Engineering, 2019, 7, 103016.	3.3	92
53	Investigation of the formation mechanisms of plasma electrolytic oxidation coatings on Mg alloy AM50 using particles. Electrochimica Acta, 2016, 196, 680-691.	2.6	91
54	Plasma anodized ZE41 magnesium alloy sealed with hybrid epoxy-silane coating. Corrosion Science, 2013, 73, 300-308.	3.0	90

#	Article	IF	CITATIONS
55	Degradation behavior of PEO coating on AM50 magnesium alloy produced from electrolytes with clay particle addition. Surface and Coatings Technology, 2015, 269, 155-169.	2.2	90
56	Interlayer intercalation and arrangement of 2-mercaptobenzothiazolate and 1,2,3-benzotriazolate anions in layered double hydroxides: In situ X-ray diffraction study. Journal of Solid State Chemistry, 2016, 233, 158-165.	1.4	90
57	Analytical characterisation and corrosion behaviour of bis-[triethoxysilylpropyl]tetrasulphide pre-treated AA2024-T3. Corrosion Science, 2005, 47, 869-881.	3.0	87
58	Bioactive plasma electrolytic oxidation coatings on Mg-Ca alloy to control degradation behaviour. Surface and Coatings Technology, 2017, 315, 454-467.	2.2	87
59	Microstructure and corrosion behavior of Ca/P coatings prepared on magnesium by plasma electrolytic oxidation. Surface and Coatings Technology, 2017, 319, 359-369.	2.2	87
60	Clarifying the decisive factors for utilization efficiency of Mg anodes for primary aqueous batteries. Journal of Power Sources, 2019, 441, 227201.	4.0	86
61	Active corrosion protection coating for a ZE41 magnesium alloy created by combining PEO and sol–gel techniques. RSC Advances, 2016, 6, 12553-12560.	1.7	84
62	Polyelectrolyte-modified layered double hydroxide nanocontainers as vehicles for combined inhibitors. RSC Advances, 2015, 5, 39916-39929.	1.7	82
63	Cerium-based sealing of PEO coated AM50 magnesium alloy. Surface and Coatings Technology, 2015, 269, 145-154.	2.2	80
64	Microâ€ <b>e</b> rc oxidation of magnesium alloys: A review. Journal of Materials Science and Technology, 2022, 118, 158-180.	5.6	79
65	Active corrosion protection of AA2024 by sol–gel coatings with cerium molybdate nanowires. Electrochimica Acta, 2013, 112, 236-246.	2.6	78
66	Sealing of tartaric sulfuric (TSA) anodized AA2024 with nanostructured LDH layers. RSC Advances, 2016, 6, 13942-13952.	1.7	76
67	A novel bilayer system comprising LDH conversion layer and sol-gel coating for active corrosion protection of AA2024. Corrosion Science, 2018, 143, 299-313.	3.0	76
68	The effect of small-molecule bio-relevant organic components at low concentration on the corrosion of commercially pure Mg and Mg-0.8Ca alloy: An overall perspective. Corrosion Science, 2019, 153, 258-271.	3.0	76
69	Ca/In micro alloying as a novel strategy to simultaneously enhance power and energy density of primary Mg-air batteries from anode aspect. Journal of Power Sources, 2020, 472, 228528.	4.0	76
70	Approaching "stainless magnesium―by Ca micro-alloying. Materials Horizons, 2021, 8, 589-596.	6.4	76
71	Synergistic corrosion inhibition on galvanically coupled metallic materials. Electrochemistry Communications, 2012, 20, 101-104.	2.3	75
72	3D reconstruction of plasma electrolytic oxidation coatings on Mg alloy via synchrotron radiation tomography. Corrosion Science, 2018, 139, 395-402.	3.0	74

#	Article	IF	CITATIONS
73	Flash-PEO as an alternative to chromate conversion coatings for corrosion protection of Mg alloy. Corrosion Science, 2021, 180, 109189.	3.0	74
74	Preparation and corrosion protective properties of nanostructured titania-containing hybrid sol–gel coatings on AA2024. Progress in Organic Coatings, 2008, 62, 226-235.	1.9	73
75	Corrosion inhibition of pure Mg containing a high level of iron impurity in pH neutral NaCl solution. Corrosion Science, 2018, 142, 222-237.	3.0	72
76	Nanocontainer-based corrosion sensing coating. Nanotechnology, 2013, 24, 415502.	1.3	70
77	Active protection of Mg alloy by composite PEO coating loaded with corrosion inhibitors. Applied Surface Science, 2020, 504, 144462.	3.1	68
78	Revealing the impact of second phase morphology on discharge properties of binary Mg-Ca anodes for primary Mg-air batteries. Corrosion Science, 2019, 153, 225-235.	3.0	67
79	Feedback active coatings based on incorporated nanocontainers. Journal of Materials Chemistry, 2006, 16, 4561-4566.	6.7	66
80	The Reduction of Dissolved Oxygen During Magnesium Corrosion. ChemistryOpen, 2018, 7, 664-668.	0.9	66
81	Layered double hydroxides (LDHs) as functional materials for the corrosion protection of aluminum alloys: A review. Applied Materials Today, 2020, 21, 100857.	2.3	65
82	Plasma electrolytic oxidation of AZ31 and AZ91 magnesium alloys: Comparison of coatings formation mechanism. Journal of Magnesium and Alloys, 2020, 8, 587-600.	5.5	64
83	Insight into physical interpretation of high frequency time constant in electrochemical impedance spectra of Mg. Corrosion Science, 2021, 187, 109501.	3.0	64
84	Anion exchange in Zn–Al layered double hydroxides: In situ X-ray diffraction study. Chemical Physics Letters, 2010, 495, 73-76.	1.2	63
85	Local pH and Its Evolution Near Mg Alloy Surfaces Exposed to Simulated Body Fluids. Advanced Materials Interfaces, 2018, 5, 1800169.	1.9	63
86	Active self-healing coating for galvanically coupled multi-material assemblies. Electrochemistry Communications, 2014, 41, 51-54.	2.3	62
87	Formation of self-lubricating PEO coating via in-situ incorporation of PTFE particles. Surface and Coatings Technology, 2018, 337, 379-388.	2.2	61
88	Microstructural influence on corrosion behavior of MgZnGe alloy in NaCl solution. Journal of Alloys and Compounds, 2019, 783, 179-192.	2.8	61
89	Corrosion inhibition of copper in aqueous chloride solution by 1H-1,2,3-triazole and 1,2,4-triazole and their combinations: electrochemical, Raman and theoretical studies. Physical Chemistry Chemical Physics, 2017, 19, 6113-6129.	1.3	60
90	Functionalized chitosan-based coatings for active corrosion protection. Surface and Coatings Technology, 2013, 226, 51-59.	2.2	59

#	Article	IF	CITATIONS
91	Chitosan as a Smart Coating for Controlled Release of Corrosion Inhibitor 2-Mercaptobenzothiazole. ECS Electrochemistry Letters, 2013, 2, C19-C22.	1.9	59
92	The effect of pulse waveforms on surface morphology, composition and corrosion behavior of Al 2 O 3 and Al 2 O 3 /TiO 2 nano-composite PEO coatings on 7075 aluminum alloy. Surface and Coatings Technology, 2017, 324, 208-221.	2.2	57
93	Active sensing coating for early detection of corrosion processes. RSC Advances, 2014, 4, 17780.	1.7	56
94	Synergetic active corrosion protection of AA2024-T3 by 2D- anionic and 3D-cationic nanocontainers loaded with Ce and mercaptobenzothiazole. Corrosion Science, 2018, 135, 35-45.	3.0	55
95	Influence of particle additions on corrosion and wear resistance of plasma electrolytic oxidation coatings on Mg alloy. Surface and Coatings Technology, 2018, 352, 1-14.	2.2	54
96	High-energy and durable aqueous magnesium batteries: Recent advances and perspectives. Energy Storage Materials, 2021, 43, 238-247.	9.5	54
97	Corrosion and discharge properties of Ca/Ge micro-alloyed Mg anodes for primary aqueous Mg batteries. Corrosion Science, 2020, 177, 108958.	3.0	53
98	Cerium cinnamate as an environmentally benign inhibitor pigment for epoxy coatings on AA 2024-T3. Progress in Organic Coatings, 2014, 77, 765-773.	1.9	52
99	Influence of surface pre-treatment on the deposition and corrosion properties of hydrophobic coatings on a magnesium alloy. Corrosion Science, 2016, 112, 483-494.	3.0	52
100	PEO coatings design for Mg-Ca alloy for cardiovascular stent and bone regeneration applications. Materials Science and Engineering C, 2019, 105, 110026.	3.8	52
101	Layered double hydroxide based active corrosion protective sealing of plasma electrolytic oxidation/sol-gel composite coating on AA2024. Applied Surface Science, 2019, 494, 829-840.	3.1	52
102	A multi-electrode cell for high-throughput SVET screening of corrosion inhibitors. Corrosion Science, 2010, 52, 3146-3149.	3.0	51
103	Comparative X-ray diffraction and infrared spectroscopy study of Zn–Al layered double hydroxides: Vanadate vs nitrate. Chemical Physics, 2012, 397, 102-108.	0.9	51
104	Corrosion behaviour of WC-10% AISI 304 cemented carbides. Corrosion Science, 2015, 100, 322-331.	3.0	51
105	Galvanic corrosion of Ti6Al4V -AA2024 joints in aircraft environment: Modelling and experimental validation. Corrosion Science, 2019, 157, 70-78.	3.0	51
106	Characterization and corrosion behavior of binary Mg-Ga alloys. Materials Characterization, 2017, 128, 85-99.	1.9	50
107	The wear characteristics of CeO2 containing nanocomposite coating made by aluminate-based PEO on AM 50 magnesium alloy. Surface and Coatings Technology, 2019, 357, 626-637.	2.2	49
108	Lanthanide Salts as Corrosion Inhibitors for AA5083. Mechanism and Efficiency of Corrosion Inhibition. Journal of the Electrochemical Society, 2008, 155, C169.	1.3	48

#	Article	IF	CITATIONS
109	Influence of sol-gel process parameters on the protection properties of sol–gel coatings applied on AA2024. Surface and Coatings Technology, 2014, 246, 6-16.	2.2	48
110	Molybdate intercalated hydrotalcite/graphene oxide composite as corrosion inhibitor for carbon steel. Surface and Coatings Technology, 2020, 399, 126165.	2.2	48
111	Localized currents and pH distribution studied during corrosion of MA8 Mg alloy in the cell culture medium. Corrosion Science, 2020, 170, 108689.	3.0	47
112	Influence of electrical parameters on particle uptake during plasma electrolytic oxidation processing of AM50 Mg alloy. Surface and Coatings Technology, 2016, 289, 179-185.	2.2	46
113	Nanoporous magnesium. Nano Research, 2018, 11, 6428-6435.	5.8	46
114	Control of the Mg alloy biodegradation via PEO and polymer-containing coatings. Corrosion Science, 2021, 182, 109254.	3.0	46
115	Surface evaluation and electrochemical behaviour of doped silane pre-treatments on galvanised steel substrates. Progress in Organic Coatings, 2007, 59, 214-223.	1.9	45
116	Performance boost for primary magnesium cells using iron complexing agents as electrolyte additives. Scientific Reports, 2018, 8, 7578.	1.6	45
117	Cerium molybdate nanowires for active corrosion protection of aluminium alloys. Corrosion Science, 2012, 58, 41-51.	3.0	44
118	Effects of graphene nanosheets on the ceramic coatings formed on Ti6Al4V alloy drill pipe by plasma electrolytic oxidation. Journal of Alloys and Compounds, 2019, 789, 996-1007.	2.8	44
119	Prediction of the internal corrosion rate for oil and gas pipeline: Implementation of ensemble learning techniques. Journal of Natural Gas Science and Engineering, 2022, 99, 104425.	2.1	44
120	Double Perovskite Sr <sub>2</sub> FeMoO <sub>6</sub> Films Prepared by Electrophoretic Deposition. ACS Applied Materials & Interfaces, 2014, 6, 19201-19206.	4.0	41
121	Zn-Al LDH growth on AA2024 and zinc and their intercalation with chloride: Comparison of crystal structure and kinetics. Applied Surface Science, 2020, 501, 144027.	3.1	41
122	EIS Study of Amine Cured Epoxy-silica-zirconia Sol-gel Coatings for Corrosion Protection of the Aluminium Alloy EN AW 6063. Portugaliae Electrochimica Acta, 2013, 31, 307-319.	0.4	40
123	Double-Ligand Strategy to Construct an Inhibitor-Loaded Zn-MOF and Its Corrosion Protection Ability for Aluminum Alloy 2A12. ACS Applied Materials & amp; Interfaces, 2021, 13, 51685-51694.	4.0	40
124	In silico screening of modulators of magnesium dissolution. Corrosion Science, 2020, 163, 108245.	3.0	38
125	The Corrosion Performance and Mechanical Properties of Mg-Zn Based Alloys—A Review. Corrosion and Materials Degradation, 2020, 1, 92-158.	1.0	38
126	MgAl-V2O7 4- LDHs/(PEI/MXene)10 composite film for magnesium alloy corrosion protection. Journal of Materials Science and Technology, 2021, 91, 28-39.	5.6	38

#	Article	IF	CITATIONS
127	A first-principles analysis of the charge transfer in magnesium corrosion. Scientific Reports, 2020, 10, 15006.	1.6	37
128	ATR-FTIR in Kretschmann configuration integrated with electrochemical cell as in situ interfacial sensitive tool to study corrosion inhibitors for magnesium substrates. Electrochimica Acta, 2020, 345, 136166.	2.6	37
129	Tailoring electrolyte additives for controlled Mg-Ca anode activity in aqueous Mg-air batteries. Journal of Power Sources, 2020, 460, 228106.	4.0	37
130	Micropotentiometric mapping of local distributions of Zn2+ relevant to corrosion studies. Electrochemistry Communications, 2010, 12, 394-397.	2.3	36
131	Photodegradation of 2-mercaptobenzothiazole and 1,2,3-benzotriazole corrosion inhibitors in aqueous solutions and organic solvents. Physical Chemistry Chemical Physics, 2014, 16, 25152-25160.	1.3	36
132	Validating the early corrosion sensing functionality in poly (ether imide) coatings for enhanced protection of magnesium alloy AZ31. Corrosion Science, 2018, 140, 307-320.	3.0	36
133	One-step synthesis and growth mechanism of nitrate intercalated ZnAl LDH conversion coatings on zinc. Chemical Communications, 2019, 55, 6878-6881.	2.2	36
134	Clarifying the influence of albumin on the initial stages of magnesium corrosion in Hank's balanced salt solution. Journal of Magnesium and Alloys, 2020, , .	5.5	36
135	Tailoring the Mg-air primary battery performance using strong complexing agents as electrolyte additives. Journal of Power Sources, 2020, 453, 227880.	4.0	36
136	Hierarchically organized Li–Al-LDH nano-flakes: a low-temperature approach to seal porous anodic oxide on aluminum alloys. RSC Advances, 2017, 7, 35357-35367.	1.7	34
137	Data Science Based Mg Corrosion Engineering. Frontiers in Materials, 2019, 6, .	1.2	34
138	Initial stages of localized corrosion at cut-edges of adhesively bonded Zn and Zn-Al-Mg galvanized steel. Electrochimica Acta, 2016, 211, 126-141.	2.6	33
139	Microstructure controls the corrosion behavior of a lean biodegradable Mg–2Zn alloy. Acta Biomaterialia, 2020, 107, 349-361.	4.1	32
140	In situ surface film evolution during Mg aqueous corrosion in presence of selected carboxylates. Corrosion Science, 2020, 171, 108484.	3.0	32
141	Recent Advances on the Application of Layered Double Hydroxides in Concrete—A Review. Materials, 2020, 13, 1426.	1.3	32
142	Plasma electrolytic oxidation of zinc alloy in a phosphate-aluminate electrolyte. Applied Surface Science, 2020, 505, 144552.	3.1	31
143	Influence of secondary phases of AlSi9Cu3 alloy on the plasma electrolytic oxidation coating formation process. Journal of Materials Science and Technology, 2020, 50, 75-85.	5.6	31
144	Mechanisms of Localized Corrosion Inhibition of AA2024 by Cerium Molybdate Nanowires. Journal of Physical Chemistry C, 2013, 117, 5811-5823.	1.5	30

#	Article	IF	CITATIONS
145	High rate oxygen reduction reaction during corrosion of ultra-high-purity magnesium. Npj Materials Degradation, 2020, 4, .	2.6	30
146	Electrochemical behaviour of the MA8 Mg alloy in minimum essential medium. Corrosion Science, 2020, 168, 108552.	3.0	30
147	A SVET investigation on the modification of zinc dust reactivity. Progress in Organic Coatings, 2008, 63, 282-290.	1.9	29
148	Electrochemical deposition of zinc from deep eutectic solvent on barrier alumina layers. Electrochimica Acta, 2015, 170, 284-291.	2.6	29
149	How Density Functional Theory Surface Energies May Explain the Morphology of Particles, Nanosheets, and Conversion Films Based on Layered Double Hydroxides. Journal of Physical Chemistry C, 2017, 121, 2211-2220.	1.5	29
150	Synergistic Mixture of Electrolyte Additives: A Route to a High-Efficiency Mg–Air Battery. Journal of Physical Chemistry Letters, 2020, 11, 8790-8798.	2.1	29
151	Biodegradation behaviour of Fe-based alloys in Hanks' Balanced Salt Solutions: Part I. material characterisation and corrosion testing. Bioactive Materials, 2022, 7, 426-440.	8.6	28
152	Volta Potential of Oxidized Aluminum Studied by Scanning Kelvin Probe Force Microscopy. Journal of Physical Chemistry C, 2010, 114, 8474-8484.	1.5	27
153	The stress corrosion cracking behaviour of biomedical Mg-1Zn alloy in synthetic or natural biological media. Corrosion Science, 2020, 175, 108876.	3.0	27
154	Corrosion behavior of Mg wires for ureteral stent in artificial urine solution. Corrosion Science, 2021, 189, 109567.	3.0	27
155	Thermal Behavior of Layered Double Hydroxide Zn–Al–Pyrovanadate: Composition, Structure Transformations, and Recovering Ability. Journal of Physical Chemistry C, 2013, 117, 4152-4157.	1.5	26
156	Influence of stripping and cooling atmospheres on surface properties and corrosion of zinc galvanizing coatings. Applied Surface Science, 2016, 389, 144-156.	3.1	26
157	Effect of unequal levels of deformation and fragmentation on the electrochemical response of friction stir welded AA2024-T3 alloy. Electrochimica Acta, 2019, 313, 271-281.	2.6	26
158	Galvanically Stimulated Degradation of Carbon-Fiber Reinforced Polymer Composites: A Critical Review. Materials, 2019, 12, 651.	1.3	26
159	Indium chloride as an electrolyte additive for primary aqueous Mg batteries. Electrochimica Acta, 2021, 373, 137916.	2.6	26
160	Investigation of electrode distance impact on PEO coating formation assisted by simulation. Applied Surface Science, 2016, 388, 304-312.	3.1	25
161	Modification of zinc powder to improve the corrosion resistance of weldable primers. Progress in Organic Coatings, 2010, 69, 184-192.	1.9	24
162	Formation of photocatalytic plasma electrolytic oxidation coatings on magnesium alloy by incorporation of TiO2 particles. Surface and Coatings Technology, 2016, 307, 287-291.	2.2	24

#	Article	IF	CITATIONS
163	Influence of water purity on the corrosion behavior of Mg0.5ZnX (X=Ca, Ge) alloys. Corrosion Science, 2019, 153, 62-73.	3.0	24
164	Exploring the corrosion inhibition mechanism of 8-hydroxyquinoline for a PEO-coated magnesium alloy. Corrosion Science, 2022, 203, 110344.	3.0	24
165	Active protective Al–Ce alloy coating electrodeposited from ionic liquid. Electrochemistry Communications, 2010, 12, 729-732.	2.3	23
166	Boron doped nanocrystalline diamond microelectrodes for the detection of Zn2+ and dissolved O2. Electrochimica Acta, 2012, 76, 487-494.	2.6	23
167	Characterisation and corrosion behaviour of plasma electrolytic oxidation coatings on high pressure die cast Mg–5Al–0.4Mn–xCe (x=0, 0.5, 1) alloys. Surface and Coatings Technology, 2015, 269, 200-211.	2.2	23
168	A computational UV–Vis spectroscopic study of the chemical speciation of 2-mercaptobenzothiazole corrosion inhibitor in aqueous solution. Theoretical Chemistry Accounts, 2016, 135, 1.	0.5	23
169	Revealing physical interpretation of time constants in electrochemical impedance spectra of Mg via Tribo-EIS measurements. Electrochimica Acta, 2022, 404, 139582.	2.6	23
170	Active Corrosion Protection by Nanoparticles and Conversion Films of Layered Double Hydroxides. Corrosion, 2014, 70, 436-445.	0.5	22
171	Interaction effect between different constituents in silicate-containing electrolyte on PEO coatings on Mg alloy. Surface and Coatings Technology, 2016, 307, 825-836.	2.2	22
172	Role of Phase Composition of PEO Coatings on AA2024 for In-Situ LDH Growth. Coatings, 2017, 7, 190.	1.2	22
173	Influence of cathodic duty cycle on the properties of tungsten containing Al 2 O 3 /TiO 2 PEO nano-composite coatings. Surface and Coatings Technology, 2018, 340, 210-221.	2.2	22
174	Enhancement of discharge performance for aqueous Mg-air batteries in 2,6-dihydroxybenzoate-containing electrolyte. Chemical Engineering Journal, 2022, 429, 132369.	6.6	22
175	A model describing the growth of a PEO coating on AM50 Mg alloy under constant voltage mode. Electrochimica Acta, 2017, 251, 461-474.	2.6	22
176	Impedance behaviour of anodic TiO2 films prepared by galvanostatic anodisation and powerful pulsed discharge in electrolyte. Electrochimica Acta, 2012, 76, 453-461.	2.6	21
177	Enhanced Wear Performance of Hybrid Epoxy-Ceramic Coatings on Magnesium Substrates. ACS Applied Materials & Interfaces, 2018, 10, 30741-30751.	4.0	21
178	Adverse effect of 2,5PDC corrosion inhibitor on PEO coated magnesium. Corrosion Science, 2021, 192, 109830.	3.0	21
179	New fluorinated diamond microelectrodes for localized detection of dissolved oxygen. Sensors and Actuators B: Chemical, 2014, 204, 544-551.	4.0	20
180	Formation of multi-functional TiO2 surfaces on AA2024 alloy using plasma electrolytic oxidation. Applied Surface Science, 2021, 544, 148875.	3.1	20

#	Article	IF	CITATIONS
181	Insight into chelating agent stimulated in-situ growth of MgAl-LDH films on magnesium alloy AZ31: The effect of initial cationic concentrations. Surface and Coatings Technology, 2022, 439, 128414.	2.2	20
182	Mechanical properties degradation of (Al-Cu-Li) 2198 alloy due to corrosion exposure. Procedia Structural Integrity, 2016, 2, 597-603.	0.3	19
183	Layered Double Hydroxide Clusters as Precursors of Novel Multifunctional Layers: A Bottom-Up Approach. Coatings, 2019, 9, 328.	1.2	19
184	Incorporation of LDH nanocontainers into plasma electrolytic oxidation coatings on Mg alloy. Journal of Magnesium and Alloys, 2023, 11, 1236-1246.	5.5	19
185	Revealing the interfacial nanostructure of a deep eutectic solvent at a solid electrode. Physical Chemistry Chemical Physics, 2020, 22, 12104-12112.	1.3	19
186	Role of phosphate, silicate and aluminate in the electrolytes on PEO coating formation and properties of coated Ti6Al4V alloy. Applied Surface Science, 2022, 595, 153523.	3.1	19
187	Novel diamond microelectrode for pH sensing. Electrochemistry Communications, 2014, 40, 31-34.	2.3	18
188	Antimicrobial activity of 2-mercaptobenzothiazole released from environmentally friendly nanostructured layered double hydroxides. Journal of Applied Microbiology, 2017, 122, 1207-1218.	1.4	18
189	Influence of SiO2 Particles on the Corrosion and Wear Resistance of Plasma Electrolytic Oxidation-Coated AM50 Mg Alloy. Coatings, 2018, 8, 306.	1.2	18
190	Difference in formation of plasma electrolytic oxidation coatings on MgLi alloy in comparison with pure Mg. Journal of Magnesium and Alloys, 2021, 9, 1725-1740.	5.5	18
191	PEO of rheocast A356 Al alloy: energy efficiency and corrosion properties. Surface and Interface Analysis, 2016, 48, 953-959.	0.8	17
192	Modification of carbon fibre reinforced polymer (CFRP) surface with sodium dodecyl sulphate for mitigation of cathodic activity. Applied Surface Science, 2019, 478, 924-936.	3.1	17
193	A comprehensive comparison of the corrosion performance, fatigue behavior and mechanical properties of micro-alloyed MgZnCa and MgZnGe alloys. Materials and Design, 2020, 185, 108285.	3.3	17
194	Self-assembled layers for the temporary corrosion protection of magnesium-AZ31 alloy. Corrosion Science, 2020, 169, 108619.	3.0	17
195	Influence of LDH conversion coatings on the adhesion and corrosion protection of friction spot-joined AA2024-T3/CF-PPS. Journal of Materials Science and Technology, 2021, 67, 197-210.	5.6	17
196	Mg Biodegradation Mechanism Deduced from the Local Surface Environment under Simulated Physiological Conditions. Advanced Healthcare Materials, 2021, 10, e2100053.	3.9	17
197	Exploring structure-property relationships in magnesium dissolution modulators. Npj Materials Degradation, 2021, 5, .	2.6	17
198	Predicting the inhibition efficiencies of magnesium dissolution modulators using sparse machine learning models. Npj Computational Materials, 2021, 7, .	3.5	17

#	Article	IF	CITATIONS
199	Barrier properties of polyurethane coil coatings treated by microwave plasma polymerization. Surface and Coatings Technology, 2006, 200, 4040-4049.	2.2	16
200	Direct Synthesis of Electrowettable Carbon Nanowall–Diamond Hybrid Materials from Sacrificial Ceramic Templates Using HFCVD. Advanced Materials Interfaces, 2017, 4, 1700019.	1.9	16
201	<i>In situ</i> kinetics studies of Zn–Al LDH intercalation with corrosion related species. Physical Chemistry Chemical Physics, 2020, 22, 17574-17586.	1.3	16
202	Experimental and quantum chemical studies of carboxylates as corrosion inhibitors for AM50 alloy in pH neutral NaCl solution. Journal of Magnesium and Alloys, 2022, 10, 555-568.	5.5	16
203	A novel lean alloy of biodegradable Mg–2Zn with nanograins. Bioactive Materials, 2021, 6, 4333-4341.	8.6	16
204	Formation of plasma electrolytic oxidation coatings on pure niobium in different electrolytes. Applied Surface Science, 2022, 573, 151629.	3.1	16
205	Corrosion and wear performance of La2O3 doped plasma electrolytic oxidation coating on pure Mg. Surface and Coatings Technology, 2022, 433, 128112.	2.2	16
206	Self-Healing Anticorrosion Coatings. , 0, , 101-139.		15
207	Corrosion behavior of metal–composite hybrid joints: Influence of precipitation state and bonding zones. Corrosion Science, 2019, 158, 108075.	3.0	15
208	Enhanced Predictive Modelling of Steel Corrosion in Concrete in Submerged Zone Based on a Dynamic Activation Approach. International Journal of Concrete Structures and Materials, 2019, 13, .	1.4	15
209	Corrosion performance, corrosion fatigue behavior and mechanical integrity of an extruded Mg4Zn0.2Sn alloy. Journal of Materials Science and Technology, 2020, 59, 107-116.	5.6	15
210	Mechanism of LDH Direct Growth on Aluminum Alloy Surface: A Kinetic and Morphological Approach. Journal of Physical Chemistry C, 2021, 125, 11687-11701.	1.5	15
211	Electrochemical deposition of lead and tellurium into barrierless nanoporous anodic aluminium oxide. Electrochimica Acta, 2012, 77, 65-70.	2.6	14
212	Melting temperature of metal polycrystalline nanowires electrochemically deposited into the pores of anodic aluminum oxide. Physical Chemistry Chemical Physics, 2014, 16, 19394.	1.3	14
213	Influence of inhibitor adsorption on readings of microelectrode during SVET measurements. Electrochimica Acta, 2019, 322, 134761.	2.6	14
214	Corrosion-induced mechanical properties degradation of Al-Cu-Li (2198-T351) aluminium alloy and the role of side-surface cracks. Corrosion Science, 2021, 183, 109330.	3.0	14
215	Biodegradation behaviour of Fe-based alloys in Hanks' Balanced Salt Solutions: Part II. The evolution of local pH and dissolved oxygen concentration at metal interface. Bioactive Materials, 2022, 7, 412-425.	8.6	14
216	Wear and corrosion behavior of clay containing coating on AM 50 magnesium alloy produced by aluminate-based plasma electrolytic oxidation. Transactions of Nonferrous Metals Society of China, 2021, 31, 3719-3738.	1.7	14

#	Article	IF	CITATIONS
217	Kelvin Microprobe Analytics on Iron-Enriched Corroded Magnesium Surface. Corrosion, 2017, 73, 583-595.	0.5	13
218	Mechanistic understanding of the corrosion behavior of Mg4Zn0.2Sn alloys: From the perspective view of microstructure. Corrosion Science, 2020, 174, 108863.	3.0	13
219	Exploring the effect of sodium salt of Ethylenediaminetetraacetic acid as an electrolyte additive on electrochemical behavior of a commercially pure Mg in primary Mg-air batteries. Journal of Power Sources, 2022, 527, 231176.	4.0	13
220	High Power Diode Laser (HPDL) surface treatments to improve the mechanical properties and the corrosion behaviour of Mg-Zn-Ca alloys for biodegradable implants. Surface and Coatings Technology, 2020, 402, 126314.	2.2	12
221	Microstructure, wear and corrosion performance of plasma electrolytic oxidation coatings formed on D16T Al alloy. Rare Metals, 2020, 39, 1425-1439.	3.6	12
222	Interplay of Superstructural Ordering and Magnetic Properties of the Sr <sub>2</sub> FeMoO <sub>6–<i>δ</i></sub> Double Perovskite. Science of Advanced Materials, 2015, 7, 446-454.	0.1	12
223	Local pH and oxygen concentration at the interface of Zn alloys in Tris-HCl or HEPES buffered Hanks' balanced salt solution. Corrosion Science, 2022, 197, 110061.	3.0	12
224	CORDATA: an open data management web application to select corrosion inhibitors. Npj Materials Degradation, 2022, 6, .	2.6	12
225	Influence of plasma electrolytic oxidation coatings on fatigue performance of AZ31 Mg alloy. Materials and Corrosion - Werkstoffe Und Korrosion, 2017, 68, 50-57.	0.8	11
226	Enhanced predictive corrosion modeling with implicit corrosion products. Materials and Corrosion - Werkstoffe Und Korrosion, 2019, 70, 2247-2255.	0.8	11
227	Effect of Heat Treatment on the Corrosion Behavior of Mg-10Gd Alloy in 0.5% NaCl Solution. Frontiers in Materials, 2020, 7, .	1.2	11
228	Evolution and performance of a MgO/HA/DCPD gradient coating on pure magnesium. Journal of Alloys and Compounds, 2021, 883, 160793.	2.8	11
229	In-situ LDHs growth on PEO coatings on AZ31 magnesium alloy for active protection: Roles of PEO composition and conversion solution. Journal of Magnesium and Alloys, 2023, 11, 2376-2391.	5.5	11
230	A critical look at interpretation of electrochemical impedance spectra of sol-gel coated aluminium. Electrochimica Acta, 2021, 378, 138091.	2.6	10
231	Zeolite-containing photocatalysts immobilized on aluminum support by plasma electrolytic oxidation. Surfaces and Interfaces, 2021, 26, 101307.	1.5	10
232	Influence of Oxygen Dissociation on the Oxidation of Iron. Oxidation of Metals, 2004, 62, 223-235.	1.0	9
233	All-Diamond Microelectrodes as Solid State Probes for Localized Electrochemical Sensing. Analytical Chemistry, 2015, 87, 6487-6492.	3.2	9
234	Aluminum Anodization in Deionized Water as Electrolyte. Journal of the Electrochemical Society, 2016, 163, C364-C368.	1.3	9

#	Article	IF	CITATIONS
235	Numerical and Experimental Analysis of Selfâ€Protection in Reinforced Concrete due to Application of Mg–Al–NO <sub>2</sub> Layered Double Hydroxides. Advanced Engineering Materials, 2020, 22, 2000398.	1.6	9
236	Sacrificial protection of Mg-based resorbable implant alloy by magnetron sputtered Mg5Gd alloy coating: A short-term study. Corrosion Science, 2021, 189, 109590.	3.0	9
237	Low interfacial pH discloses the favorable biodegradability of several Mg alloys. Corrosion Science, 2022, 197, 110059.	3.0	9
238	Role of cobalt additive on formation and anticorrosion properties of PEO coatings on AA2024 alloy in alkali-silicate electrolyte. Surface and Coatings Technology, 2022, 433, 128075.	2.2	9
239	Atomistic Insight into the Hydration States of Layered Double Hydroxides. ACS Omega, 2022, 7, 12412-12423.	1.6	9
240	Fast coating of ultramicroelectrodes with boron-doped nanocrystalline diamond. Diamond and Related Materials, 2010, 19, 1330-1335.	1.8	8
241	Digital modelling of the galvanic corrosion behaviour of a self–piercing riveted AZ31 ―AA5083 hybrid joint. Materialwissenschaft Und Werkstofftechnik, 2017, 48, 529-545.	0.5	8
242	Mg Alloys: Challenges and Achievements in Controlling Performance, and Future Application Perspectives. Minerals, Metals and Materials Series, 2018, , 3-14.	0.3	8
243	The Influence of PSA Pre-Anodization of AA2024 on PEO Coating Formation: Composition, Microstructure, Corrosion, and Wear Behaviors. Materials, 2018, 11, 2428.	1.3	8
244	Simulation assisted investigation of substrate geometry impact on PEO coating formation. Surface and Coatings Technology, 2018, 350, 281-297.	2.2	8
245	Effect of Surface Pre-Treatments on the Formation and Degradation Behaviour of a Calcium Phosphate Coating on Pure Magnesium. Coatings, 2019, 9, 259.	1.2	8
246	Corrosion Inhibition and Acceleration by Rare Earth Ions in Galvanic Couples. Journal of the Electrochemical Society, 2019, 166, C642-C648.	1.3	8
247	Insights into corrosion behaviour of uncoated Mg alloys for biomedical applications in different aqueous media. Journal of Materials Research and Technology, 2021, 13, 1908-1922.	2.6	8
248	Evaluation of the biodegradation product layer on Mg-1Zn alloy during dynamical strain. Journal of Magnesium and Alloys, 2021, 9, 1820-1833.	5.5	8
249	PEO processing of AZ91Nd/Al2O3 MMC-the role of alumina fibers. Journal of Magnesium and Alloys, 2022, 10, 423-439.	5.5	8
250	Surface modification of coil coatings with thin plasma polymer films structure and stability. Progress in Organic Coatings, 2007, 58, 248-252.	1.9	7
251	Anodic Alumina Films Prepared by Powerful Pulsed Discharge Oxidation. Journal of Physical Chemistry C, 2011, 115, 18634-18639.	1.5	7
252	Effect of the Anodic Titania Layer Thickness on Electrodeposition of Zinc on Ti/TiO <sub>2</sub> from Deep Eutectic Solvent. Journal of the Electrochemical Society, 2017, 164, D88-D94.	1.3	7

#	Article	IF	CITATIONS
253	The effect of grain boundary precipitates on stress corrosion cracking in a bobbin tool friction stir welded Al-Cu-Li alloy. Materials Letters: X, 2019, 2, 100014.	0.3	7
254	Properties of ZnO/ZnAl2O4 composite PEO coatings on zinc alloy Z1. Surface and Coatings Technology, 2021, 410, 126948.	2.2	7
255	Formation and corrosion behaviors of calcium phosphate coatings on plasma electrolytic oxidized Mg under changing chemical environment. Surface and Coatings Technology, 2021, 412, 127030.	2.2	7
256	Bilayer coatings for temporary and long–term corrosion protection of magnesium–AZ31 alloy. Progress in Organic Coatings, 2022, 163, 106608.	1.9	7
257	In situ synergistic strategy of sacrificial intermedium for scalable-manufactured and controllable layered double hydroxide film. Science China Materials, 2022, 65, 1842-1852.	3.5	7
258	Influence of the RF plasma polymerization process on the barrier properties of coil-coating. Progress in Organic Coatings, 2005, 53, 225-234.	1.9	6
259	Titania Films Obtained by Powerful Pulsed Discharge Oxidation in Phosphoric Acid Electrolytes. Journal of the Electrochemical Society, 2014, 161, D73-D78.	1.3	6
260	Smallâ€Angle Neutron Scattering and Magnetically Heterogeneous State in Sr 2 FeMoO 6–δ. Physica Status Solidi (B): Basic Research, 2019, 256, 1800428.	0.7	6
261	Anticorrosion thin film smart coatings for aluminum alloys. , 2020, , 429-454.		6
262	Magnetic Properties of La0.9A0.1MnO3 (A: Li, Na, K) Nanopowders and Nanoceramics. Materials, 2020, 13, 1788.	1.3	6
263	CHAPTER 12. Aqueous Mg Batteries. RSC Energy and Environment Series, 2019, , 275-308.	0.2	6
264	Role of polymorph microstructure of Ti6Al4V alloy on PEO coating formation in phosphate electrolyte. Surface and Coatings Technology, 2021, 428, 127890.	2.2	6
265	Controllable Degradable Plasma Electrolytic Oxidation Coated Mg Alloy for Biomedical Application. Frontiers in Chemical Engineering, 2022, 4, .	1.3	6
266	A mathematical model describing the surface evolution of Mg anode during discharge of aqueous Mg-air battery. Journal of Power Sources, 2022, 542, 231745.	4.0	6
267	"Superpermeability―and "pumping―of atomic hydrogen through palladium membranes. Journal of Membrane Science, 2008, 320, 528-532.	4.1	5
268	Influence of pH on the Corrosion Protection of Epoxy-Silica-Zirconia Sol-Gel Coatings Applied on EN AW-6063 Aluminium Alloy. ECS Transactions, 2014, 58, 9-16.	0.3	5
269	Electrodeposition of Zinc Nanorods from Ionic Liquid into Porous Anodic Alumina. ChemElectroChem, 2014, 1, 1484-1487.	1.7	5
270	Enhanced predictive corrosion modeling via randomly distributed boundary conditions. Materials and Corrosion - Werkstoffe Und Korrosion, 2018, 69, 1720-1728.	0.8	5

#	Article	IF	CITATIONS
271	The Stability and Chloride Entrapping Capacity of ZnAl-NO2 LDH in High-Alkaline/Cementitious Environment. Corrosion and Materials Degradation, 2021, 2, 78-99.	1.0	5
272	Dielectric barrier formation and tunneling magnetoresistance effect in strontium iron molybdate. Technical Physics Letters, 2013, 39, 552-555.	0.2	4
273	Evaporation of Electrolyte during SVET Measurements: The Scale of the Problem and the Solutions. Electroanalysis, 2019, 31, 2290-2298.	1.5	4
274	The Influence of In Situ Anatase Particle Addition on the Formation and Properties of Multifunctional Plasma Electrolytic Oxidation Coatings on AA2024 Aluminum Alloy. Advanced Engineering Materials, 2021, 23, 2001527.	1.6	4
275	Modification of Porous Titania Templates for Uniform Metal Electrodeposition from Deep Eutectic Solvent. Journal of the Electrochemical Society, 2017, 164, D335-D341.	1.3	3
276	Self-cleaning property of AZ31 Mg alloy during plasma electrolytic oxidation process. Progress in Natural Science: Materials International, 2019, 29, 94-102.	1.8	3
277	Interoperability architecture for bridging computational tools: application to steel corrosion in concrete. Modelling and Simulation in Materials Science and Engineering, 2020, 28, 025003.	0.8	3
278	Effect of 6-Aminohexanoic Acid Released from Its Aluminum Tri-Polyphosphate Intercalate (ATP-6-AHA) on the Corrosion Protection Mechanism of Steel in 3.5% Sodium Chloride Solution. Corrosion and Materials Degradation, 2021, 2, 666-677.	1.0	3
279	Stability of Thin Plasma Polymer Films Applied on Coil Coatings. Plasma Processes and Polymers, 2006, 3, 618-626.	1.6	2
280	Charge transfer processes and magnetoresistance in strontium ferromolybdate with dielectric barriers. Physica Status Solidi (B): Basic Research, 2013, 250, 825-830.	0.7	2
281	High-pressure induced phase formation in the CuGaS2-CuGaO2chalcopyrite-delafossite system. Physica Status Solidi (B): Basic Research, 2014, 251, 1192-1196.	0.7	2
282	Highâ€pressure zinc oxysulphide phases in the ZnO–ZnS system. Physica Status Solidi (A) Applications and Materials Science, 2015, 212, 791-795.	0.8	2
283	Environmentally friendly anodising process for structural bonding of titanium. Materialwissenschaft Und Werkstofftechnik, 2016, 47, 400-408.	0.5	2
284	Introduction of an innovative corrosion-protective alkyd steel coating based on a novel layered aluminum tripolyphosphate loaded with 6-amino hexanoic acid (ATP-6-AHA). Progress in Organic Coatings, 2021, 161, 106500.	1.9	2
285	Semiconducting properties of surface-treated titanium and their effect on peel resistance: Experimental and modelling studies. International Journal of Adhesion and Adhesives, 2022, 113, 103049.	1.4	2
286	AFM Study of the Corrosion of Pipeline Steel in Organic Compounds Extracted from Soil. ECS Transactions, 2007, 11, 107-119.	0.3	1
287	4. Protection of multimaterial assemblies. , 2015, , 73-102.		1
288	Predictive modeling of mechanical properties of metal filled anodic aluminum oxide. Journal of Mechanics of Materials and Structures, 2016, 11, 583-594.	0.4	1

#	Article	IF	CITATIONS
289	Smart Protection of Carbon-Reinforced Composite Materials and CFRP-Metal Joints. , 2021, , 429-449.		1
290	Sol-Gel Coatings with Nanocontainers of Corrosion Inhibitors for Active Corrosion Protection of Metallic Materials. , 2018, , 2435-2471.		1
291	Two Thermodynamics-Based Approaches to Atomic Oxygen Sensing. Journal of Spacecraft and Rockets, 2006, 43, 426-430.	1.3	0
292	Effect of Inorganic Content on the Performance of Anticorrosive Hybrid Sol-Gel Coated EN AW-6063 Alloy. Materials Science Forum, 2012, 730-732, 745-750.	0.3	0
293	Composite Materials: Direct Synthesis of Electrowettable Carbon Nanowall–Diamond Hybrid Materials from Sacrificial Ceramic Templates Using HFCVD (Adv. Mater. Interfaces 10/2017). Advanced Materials Interfaces, 2017, 4, .	1.9	0
294	Encapsulation of Al and Ti-Al alloy 1-D nanorods into oxide matrix by powerful pulsed discharge method. Journal of Solid State Electrochemistry, 2018, 22, 3913-3920.	1.2	0